nostaining with antibodies to glial fibrillary acidic protein (GFAP), a marker of glial differentiation, confirmed that astrotactin both conferred glial binding and induced glial differentiation (Table 1). In control experiments, purified glial cells did not bind to untransfected 3T3 cells. These experiments demonstrate that the mode of action of astrotactin is to provide a heterophilic ligand for glial binding. As a secondary effect, astrotactin appears to maintain the differentiation of glial cells.

The mechanism of action of astrotactin seen in assays in vitro is consistent with the structure of the protein. EGF repeats have been implicated in cell-cell signaling (*11*), suggesting that astrotactin functions in a signaling pathway that is crucial for neuron-glia interactions before and during migration. Because glial cells bind to neurons and undergo differentiation in response to astrotactin, we anticipate an astrotactin receptor on the glial surface. With the cloning of the gene encoding astrotactin, at least three genes can be proposed to function in the migration and assembly of neurons during murine cortical histogenesis: (i) *Weaver* acts at the earliest stage, blocking the expression of a ligand needed for entry of postmitotic neurons into a program of gene expression that includes expression of astrotactin and TAG1 (*17*). (ii) The gene encoding astrotactin is expressed in initial steps of differentiation required for utilization of the glial scaffold for migration and laminar formation. (iii) *Reelin* acts at later steps, during the arrest of locomotion of the migrating neuron along glial fibers and formation of neuronal layers (*10*, *18*).

REFERENCES AND NOTES

1. S. Ramon y Cajal, *Histologie du Système Nerveux de l'Homme et des Vertebres* (Maloine, Paris, 1911; reprinted by Consejo Superior de Investigaciones Cientificas, Madrid).
2. P. Rakic, *Brain Res.* **33**, 471 (1971); *J. Comp. Neurol.* **141**, 283 (1971); *ibid.*, **145**, 61 (1972).
3. J. C. Edmondson and M. E. Hatten, *J. Neurosci.* **7**, 1928 (1987); M. E. Hatten, *Curr. Opin. Neurobiol.* **3**, 38 (1993).
4. G. Fishell and M. E. Hatten, *Development* **113**, 755 (1991).
5. T. N. Stitt and M. E. Hatten, *Neuron* **5**, 639 (1990).
6. S. Kuhar *et al.*, *Development* **112**, 97 (1993).
7. To obtain cDNAs encoding the 5′ end of the astrotactin protein, a randomly primed, P5 cerebellar granule cell cDNA library was constructed in the γ plasmid λZAPII vector. The 5′ GC14 cDNA fragment was used to screen this library. GC14 cDNAs were also isolated from a P20 mouse brain oligo(dT) λZAPII cDNA library (J. Friedman, Rockefeller University).
8. R. M. Cooke *et al.*, *Nature* **327**, 339 (1987).
9. K. Skorstengaard, M. S. Jesen, P. Sdahl, T. E. Petersen, S. Magnusson, *Eur. J. Biochem.* **161**, 441 (1986).
10. G. D'Arcangelo *et al.*, *Nature* **374**, 719 (1995).
11. I. Greenwald, *Curr. Opin. Genet. Dev.* **4**, 556 (1994).
12. T. M. Jessell, *Neuron* **1**, 3 (1988).
13. Total RNA was purified from various tissues with the use of the RNAZol method (Gel-test, Inc.). Complementary DNA probes were derived from the GC14 3′ noncoding region. As a control, the blots were hybridized with a glyceraldehyde-3-phosphate dehydrogenase probe.
14. To produce recombinant GC14 protein, a cDNA fragment containing the region of one EGF and one FNIII repeat was subcloned into pGEM-3X vector (Pharmacia). Affinity purification of antibodies to GC14 was according to the protocol in *Current Protocols in Molecular Biology*, F. M. Ausubel *et al.*, Eds. (Wiley, New York, 1994), vol. 2, suppl. 27. Cell culture experiments were carried out with primary cells from cerebellums harvested on postnatal days 5 to 6. The in vitro migration culture assay was performed as described previously. Fab fragments prepared from these antibodies were added at a concentration of 0.4 μg/ml. Cell images were recorded with a Panasonic optical memory disk recorder, and measurements of neuronal migration were made with Metamorph software (Universal Imaging).
15. Full-length GC14 cDNA was subcloned into pRC/CMV vector (Invitrogen) and transfected into 3T3 cells by calcium phosphate–mediated gene transfer. Colonies resistant to G418 were screened for astrotactin expression by protein immunoblot. As a control, cell lines containing the vector alone were also tested. For the cell-binding assay, a monolayer of 3T3 cells was preplated. Granule and glial cells were labeled with PKH26 dye and added to the 3T3 cells. After 36 hours in vitro, the number of the labeled cells that bound and the percentage of bound cells that were differentiated were quantified by random counting of cells in 10 fields at a magnification of ×20.
16. A. J. Furley *et al.*, *Cell* **61**, 157 (1990).
17. W. Q. Gao, X. L. Liu, M. E. Hatten *ibid.* **68**, 841 (1992); W. Q. Gao and M. E. Hatten, *Science* **260**, 367 (1993).
18. V. S. Caviness Jr. and R. L. Sidman, *J. Comp. Neurol.* **148**, 141 (1973).

19. G. Fishell and L. Feng provided critical assistance with the experiments reported in Fig. 3. We gratefully acknowledge the advice of C. Mason, E. Ross, and K. Zimmerman throughout these experiments. C.Z. thanks G. Dietz for many helpful discussions and for assistance in the final characterization of the astrotactin cDNAs. S. Kuhar, L. Feng, X.-L. Liu, E. Ross, and S. Vidan participated in the identification of the original set of cDNA clones used in this study; randomly primed granule cell cDNA libraries were supplied by X.-M. Qian, and D. Patterson provided expert technical assistance with in situ hybridization and photomicroscopy. Supported by NIH grant NS15429 (M.E.H.) and a McKnight Neuroscience Award (M.E.H.).

8 December 1995; accepted 7 February 1996

Circadian Rhythms in Cultured Mammalian Retina

Gianluca Tosini and Michael Menaker*

Many retinal functions are circadian, but in most instances the location of the clock that drives the rhythm is not known. Cultured neural retinas of the golden hamster (*Mesocricetus auratus*) exhibited circadian rhythms of melatonin synthesis for at least 5 days at 27°C. The rhythms were entrained by light cycles applied in vitro and were free-running in constant darkness. Retinas from hamsters homozygous for the circadian mutation *tau*, which shortens the free-running period of the circadian activity rhythm by 4 hours, showed a shortened free-running period of melatonin synthesis. The mammalian retina contains a genetically programmed circadian oscillator that regulates its synthesis of melatonin.

Virtually all organisms have circadian (about 24-hour) rhythms that are driven by endogenous oscillators. In nonmammalian vertebrates, circadian oscillators have been identified in the pineal organ (*1*), the retina (*2*), and tentatively the hypothalamus (*3*). In mammals, only the suprachiasmatic nucleus of the hypothalamus (SCN) has been proven to contain circadian oscillators (*4*), although there is indirect evidence that they may exist in the retina as well (*5*).

Researchers at several laboratories including our own have failed to demonstrate circadian rhythmicity of melatonin synthesis in mammalian retinas cultured at 37°C. However, because golden hamsters (*M. auratus*) are hibernators, their tissues tolerate lowered culture temperatures, and we therefore attempted to culture their neural retinas at a constant temperature of 27°C. In chambers identical to those used for *Xenopus* retina (*6*), the hamster retinas were continuously perifused with medium at 0.5 ml/hour. Medium was collected with a fraction collector at 3-hour intervals and radioimmunoassayed for melatonin (*7*).

In a light:dark cycle (LD 14:10; light intensity of 1800 μW/cm^2) cultured hamster retinas were robustly rhythmic for the duration of the experiment (4 days), with period lengths of 24 hours and peaks of melatonin synthesis during the dark phase of the cycle (Fig. 1, A and B); the hamster retinas exhibited the same general pattern as that found in the cultured retina of *Xenopus* (*2*) and in cultured pineal glands of many nonmammalian vertebrates (*1*). In most of these other systems, light directly suppresses melatonin synthesis. In our experiments such suppression, if it occurs, is not complete (Fig. 2, A and B).

The rhythm of melatonin synthesis can be entrained in vitro (Fig. 2). Three retinas were cultured in a light cycle that was advanced 7 hours from the cycle of the intact animals, and three other retinas were cultured in a light cycle that was 7 hours

Department of Biology and National Science Foundation Center for Biological Timing, University of Virginia, Charlottesville, VA 22903, USA.

*To whom correspondence should be addressed.

Table 1. Characteristics of the circadian rhythm of melatonin synthesis from cultured retinas of wild-type (animals 1 through 4) and *tau* mutant (animals 5 through 8) hamsters.

Hamster number	Mean melatonin release (pg/ml)	Range of melatonin values (pg/hour), minimum–maximum	Free-running period (τ) (*10*) (hours)
1	52.1	0–159	23.6
2	82.0	41–238	24.5
3	60.7	16–150	23.9
4	56.4	0–156	23.5
Average period of wild-type retinas			23.87 (23.99)*
5	52.7	14–127	21.1
6	51.2	12–189	20.0
7	54.6	20–106	22.1
8	60.4	18–158	21.7
Average period of *tau* mutant retinas			21.22 (20.17)*

*Average free-running period of intact animals' locomotor rhythms (see text).

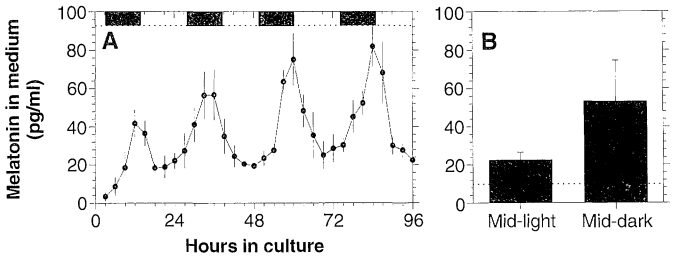

Fig. 1. (**A**) Average melatonin synthesis (± SEM) by four wild-type hamster neural retinas cultured individually in a light:dark cycle (black and white bars) at 27°C. Retinas were removed and placed in culture 3 hours before the first point on the graph. The light cycle to which the retinas were exposed was identical [except for intensity, which was 1800 μW/cm^2 in the culture chamber (*11*) and 300 μW/cm^2 in the animal's cage] with the light cycle to which the animals had been exposed previously. (**B**) Average mid-light and mid-dark melatonin values (± SEM) from the data set in (A). There is a significant difference ($P < 0.01$). The mid-light values are above the limit of detectability of the assay (dotted line).

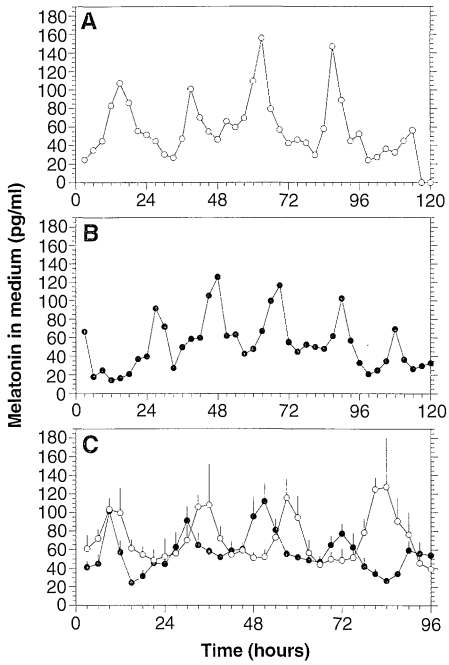

Fig. 3. Rhythms of melatonin synthesis from single neural retinas of (**A**) wild-type and (**B**) homozygous *tau* mutant hamsters cultured at 27°C in constant darkness. (**C**) Free-running rhythms of melatonin synthesis by wild-type and *tau* mutant retinas. The data (mean ± SEM) are from four wild-type hamster retinas (open circles) and four homozygous mutant hamster retinas (filled circles), and the two data sets were normalized to the time of the first peak (see also Table 1).

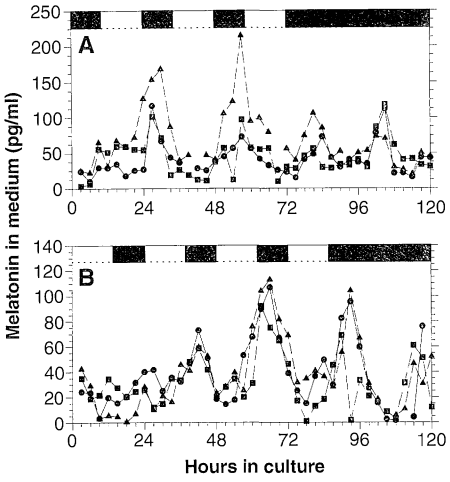

Fig. 2. Entrainment of retinal melatonin synthesis by light in vitro. Three wild-type hamsters were held on LD 14:10 and killed in the middle of the light. Neural retinas were cultured at 27°C in two different light cycles: (**A**) Retinas from the right eyes were phase-advanced by 7 hours relative to the previous cycle and (**B**) retinas from the left eyes were phase-delayed by 7 hours relative to the previous cycle for three cycles and then released into DD (black and white bars). Individual curves for each of the six retinas are plotted. The light intensity in this experiment (3000 μW/cm^2) does not completely suppress melatonin synthesis by the retina.

delayed. When they were released into constant darkness three cycles later, the melatonin peaks of the two groups were roughly in antiphase.

In constant darkness (DD), the rhythms of melatonin synthesis by cultured hamster retinas persisted for the duration of our experiments (five to six circadian cycles), demonstrating that this mammalian retina contains one or more circadian clocks that function independently of the SCN (Fig. 3, A through C). The periods of the retinal rhythms reflected the genotype of the animals from which the retinas were derived (Table 1 and Fig. 3); retinas from wild-type hamsters had periods ranging from 23.5 to 24.5 hours (average, 23.9 hours), whereas retinas from hamsters homozygous for the *tau* gene had periods ranging from 20.0 to 22.1 hours (average, 21.2 hours). The period of the locomotor activity rhythm of wild-type hamsters in our laboratory averaged 23.99 hours (average of 70 animals), whereas that of *tau* mutants averaged 20.17 hours (average of 53 animals). The retinal clock of the golden hamster therefore fulfills all the major criteria that define circadian oscillators: (i) It can be entrained; (ii) it is free-running under constant conditions; and (iii) because its period is still in the circadian range at 27°C, it must be temperature-compensated. Thus, mammals have at least two circadian oscillators, one in the SCN and one in the retina.

In our earlier work we established that the period of the circadian oscillator within the SCN is modified by the *tau* gene (*8*). The results presented here demonstrate that this gene also modifies the period of the circadian oscillator within the retina. Although as yet we do not know the molecular basis of this gene's effects, it must act on a general circadian process rather than on a specific property of the SCN.

Our results demonstrate directly that (i) the neural retina of a mammal synthesizes melatonin; (ii) a mammalian retina contains one or more circadian oscillators that regulate melatonin synthesis and perhaps other retinal processes as well; (iii) these circadian oscillators can be entrained directly by light cycles; and (iv) the period of the retinal circadian oscillators is influenced by the *tau* gene in the same way that this gene influences the period of the circadian oscillators in the SCN. Our data leave open the question of whether retinal melatonin synthesis in mammals, like that in photosensitive pineals of nonmammalian vertebrates, can be directly suppressed by light.

There are numerous reports of melatonin rhythmically synthesized by cultured pineal glands of nonmammalian vertebrates (*1*), and we have recently detected rhythmic melatonin synthesis in the cultured retinas and parietal eyes of the lizard *Iguana iguana* and in cultured retinas of lamprey (*Petromyzon marinus*) (9). Taken together, these observations suggest that all organized vertebrate photoreceptive structures synthesize melatonin under the control of circadian oscillators. It is an obvious corollary of this hypothesis that melatonin, and more specifically, circadian rhythmicity of melatonin level, is essential for normal photoreceptor function.

REFERENCES AND NOTES

1. M. Menaker and S. Wisner, *Proc. Natl. Acad. Sci. U.S.A.* **80**, 6119 (1983); J. S. Takahashi, N. Murakami, S. S. Nikaido, B. L. Pratt, L. M. Robertson, *Recent Progr. Horm. Res.* **45**, 279 (1989); J. Falcon and J. P. Collins, *Cell Tissue Res.* **265**, 601 (1991).
2. G. M. Cahill and J. C. Besharse, *Prog. Retinal Eye Res.* **14**, 267 (1995).
3. J. S. Takahashi and M. Menaker, *J. Neurosci.* **2**, 815 (1982); D. S. Janik, G. E. Pickard, M. Menaker, *J. Comp. Physiol. A* **166**, 811 (1990); S. Ooka-Souda, T. Kadota, H. Kabasawa, *Neurosci. Lett.* **164**, 33 (1993).
4. D. K. Welsh, D. E. Logothetis, M. Meister, S. M. Reppert, *Neuron* **14**, 697 (1995).
5. M. Terman and J. Terman, *Ann. N.Y. Acad. Sci.* **453**, 147 (1985); C. E. Reme, A. Wirz-Justice, M. Terman, *J. Biol. Rhythms* **6**, 5 (1991); J. S. Terman, C. E. Reme, M. Terman, *Brain Res.* **605**, 256 (1993).
6. G. M. Cahill and J. C. Besharse, *J. Neurosci.* **11**, 2959 (1991).
7. We used a modification of the method of M. Rollag and G. Niswender [*Endocrinology* **98**, 482 (1976)]. The lower limits of the assay were 1.8 to 2.5 pg per tube, and the upper limits were 500 pg per tube.
8. M. R. Ralph and M. Menaker, *Science* **241**, 1225 (1988); M. R. Ralph, R. G. Foster, F. C. Davis, M. Menaker, *ibid.* **247**, 975 (1990).
9. M. Menaker and G. Tosini, in *Sixth Sapporo Symposium on Biological Rhythm*, T. Hiroshige and K. Honma, Eds. (Hokkaido Univ. Press, Sapporo, Japan, in press).
10. Analysis of the time-series data was performed by an iterative, coupled Fourier transform–nonlinear least squares estimation procedure developed at the National Science Foundation Center for Biological Timing at the University of Virginia [M. L. Johnson and S. G. Frasier, *Methods Enzymol.* **117**, 301 (1985); M. Straume, S. G. Frasier-Cadoret, M. L. Johnson, in *Topics in Fluorescence Spectroscopy: Principles*, J. R. Lakowicz, Ed. (Plenum, New York, 1991), vol. 2, p. 177]. This software is available from the National Science Foundation Center for Biological Timing at the University of Virginia.
11. A fiber optic light powered by a 150-W tungsten quartz-halogen lamp was used in the experiments in which the cultured retinas were exposed to L:D cycles. The light source was located outside the incubator, and the tip of the fiber-optic probe was inside the incubator about 15 cm from the plate containing the cultures. We estimated light intensities at the level of the retinas by placing an irradiance detector of a UDT 350 radiometer-photometer (United Detector Technology, Hawthorne, CA) at the same location as the superfusion chamber.

12. Supported by International Human Frontier Science Program fellowship (LT-145/93) to G.T. and NIH grant (HD-13162) to M.M. We thank M. Straume for the statistical analysis, G. Cahill for discussion, and M. Rollag for the melatonin antibody.

2 November 1995; accepted 8 February 1996

Requirement for α-CaMKII in Experience-Dependent Plasticity of the Barrel Cortex

Stanislaw Glazewski,* Chuan-Min Chen, Alcino Silva, Kevin Fox†

The mammalian sensory neocortex exhibits experience-dependent plasticity such that neurons modify their response properties according to changes in sensory experience. The synaptic plasticity mechanism of long-term potentiation requiring calcium-calmodulin–dependent kinase type II (CaMKII) could underlie experience-dependent plasticity. Plasticity in adult mice can be induced by changes in the patterns of tactile input to the barrel cortex. This response is strongly depressed in adult mice that lack the gene encoding α-CaMKII, although adolescent animals are unaffected. Thus, α-CaMKII is necessary either for the induction or for the expression of plasticity in adult mice.

In mammals, the somatosensory cortex contains a complete map of the body surface. The map is capable of undergoing functional reorganization in response to manipulations of the periphery (*1*, *2*). In rodents, experience of the world through a single whisker, rather than the normal array of five rows of whiskers, results in increased representation of the spared vibrissa in the cortex (*3*, *4*). Vibrissa deprivation plasticity has a number of properties in common with ocular dominance plasticity in the visual cortex, including a critical period for plasticity within cortical layer IV and a longer period for plasticity in layers II and III (*4*, *5*).

The molecular mechanisms that underlie experience-dependent plasticity remain unclear. Plasticity could be achieved if a molecular switch, such as an autophosphorylating kinase, were located at the synapse (*6*, *7*). The abundant postsynaptic protein calcium-calmodulin–dependent kinase type II (CaMKII) has the appropriate properties (*7*, *8*). Indeed, some forms of synaptic plasticity, such as long-term potentiation (LTP) in the hippocampus, are dependent on

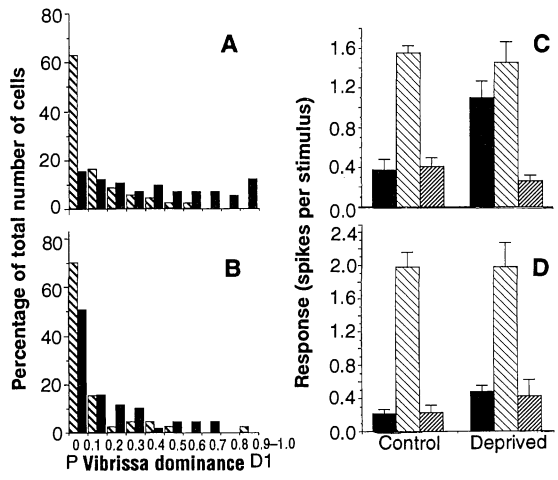

Fig. 1. Plasticity in normal adult mouse neocortex induced by vibrissa deprivation. (**A** and **B**) Pooled data for cells recorded in barrel columns immediately surrounding D1. In undeprived mice (hatched bars, 95 neurons) the VDH (*16*) was biased toward the principal vibrissa (P), and most cells showed no response to the D1 vibrissa. After deprivation (black bars, 118 neurons), the distribution shifted toward the spared vibrissa (D1) in layers II and III (A), such that 32% of neurons showed greater responses to D1 than to the principal vibrissa. The effect was less pronounced in layer IV (B), where 50% still showed no response to D1. The WVDI estimates variations in VDHs between animals (*16*) and changed significantly for cells in layers II and III after deprivation (A) (control mean ± SD = 0.11 ± 0.09; deprived mean = 0.51 ± 0.19, $P < 0.05$, *t* test) but not for cells in layer IV (B) (control mean = 0.10 ± 0.09; deprived mean = 0.17 ± 0.14, $P > 0.1$, *t* test). (**C** and **D**) The absolute response magnitude is plotted for three vibrissa types: the spared D1 vibrissa (solid bars), deprived principal vibrissa (wide hatch marks), and deprived surround receptive field vibrissa (narrow hatch marks) (*16*). In layers II and III (C), the average D1 response magnitude increased almost threefold with deprivation (control mean ± SD = 0.37 ± 0.29 spikes per stimulus; deprived mean = 1.1 ± 0.47) [ANOVA, $F(1,14) = 6.5$, $P = 0.024$]. The average principal vibrissa response did not change significantly (control = 1.57 ± 0.19; deprived = 1.46 ± 0.58) [$F(1,14) = 0.80$, $P = 0.38$] nor did responses of surround vibrissae (control = 0.41 ± 0.23 and deprived = 0.26 ± 0.17) [$F(1,13) = 2.5$, $P = 0.14$]. In layer IV (D), deprivation did not cause a change in the principal vibrissa response (control mean = 1.98 ± 0.49 spikes per stimulus; deprived mean = 1.98 ± 0.77). But there was a small but significant increase in the D1 vibrissa response (control mean ± SD = 0.22 ± 0.15; deprived mean = 0.48 ± 0.20) [$F(1,13) = 8.4$, $P = 0.013$], although no significant change in the surround deprived vibrissa response (control mean = 0.23 ± 0.23; deprived mean = 0.42 ± 0.54) [$F(1,11) = 0.55$, $P = 0.47$]. The histograms show means and standard errors calculated across animals.